Construction of a High-Density Genetic Linkage Map and QTL Mapping for Stem Rot Resistance in Passion Fruit (Passiflora edulis)

Yanyan Wu , Weihua Huang , Jieyun Liu , Junniu Zhou , Qinglan Tian , Xiuzhong Xia , Haifei Mou * , Xinghai Yang *

Posted Date: 28 October 2024

doi: 10.20944/preprints202410.2200.v1

Keywords: Passion fruit ; Single nucleotide polymorphisms ; Genetic map ; Linkage analysis ; Stem rot resistance ; Candidate gene

 doi:10.20944/preprints202410.2200.v1

Article

Construction of a High-Density Genetic Linkage Map and QTL Mapping for Stem Rot Resistance in Passion Fruit (*Passiflora edulis*)

Yanyan Wu [1], Weihua Huang [1], Jieyun Liu [1], Qinglan Tian [1], Junniu Zhou [1], Xiuzhong Xia [2], Haifei Mou [1,*] and Xinghai Yang [2,*]

[1] Biotechnology Research Institute, Guangxi Academy of Agricultural Sciences, Nanning 530007, China

[2] Guangxi Key Laboratory of Rice Genetics and Breeding, Rice Research Institute, Guangxi Academy of Agricultural Sciences, Nanning 530007, China

* Correspondence: yangxinghai514@163.com; Tel: +867713244040; mhf@gxaas.net; Tel: +86771 3245832

Abstract: The cultivated passion fruit (*Passiflora edulis*) is a diploid plant (2n=2x=18) and is an important fruit tree in southern China. However, the occurrence and spread of stem rot in passion fruit severely impact its yield and quality. This study aims to construct a high-density genetic linkage map and identify the quantitative trait locus (QTL) and candidate genes associated with stem rot resistance in passion fruit. In this study, we used an HG and ZG7 hybrid to develop a BC_1F_1 population consisting of 158 individuals. Take a previously published passion fruit genome as reference, a high-density genetic linkage map was constructed with 1,180,406 single nucleotide polymorphisms (SNPs). The map contains 9 linkage groups, covering a total genetic distance of 1559.03 cM, with an average genetic distance of 311.81 cM. The average genetic distance between 4206 bins was 0.404 cM, and the average gap length was 10.565 cM. The collinearity correlation coefficient between the genetic map and the passion fruit genome was 0.9994. *Fusarium solani* was used to infect the BC_1F_1 population, and the resistance to stem rot showed a continuous distribution. A QTL, *qPSR5*, was identified in the 145.878-152.951 cM region on the 5th linkage group. We performed RNA-seq and RT-qPCR to analyze the expression levels of predicted genes in the candidate region and identified *ZX.05G0020740* and *ZX.05G0020810* as ideal candidate genes for stem rot resistance in passion fruit. The findings in this study not only lay the foundation for cloning the *qPSR5* responsible for stem rot resistance but also provide genetic resources for the genetic improvement of passion fruit.

Keywords: Passion fruit; Single nucleotide polymorphisms; Genetic map; Linkage analysis; Stem rot resistance; Candidate gene

1. Introduction

The cultivated passion fruit is a herbaceous vine plant, known for its aromatic fruit, which is rich in sugars, vitamins, and essential minerals such as calcium, iron, and zinc, offering high nutritional value. However, stem rot, caused by fungi such as *Fusarium oxysporum* and *Fusarium solani*, has been spreading in southern China, significantly affecting the yield and quality of passion fruit. Studies have shown that using molecular breeding techniques to develop disease-resistant varieties is the most effective and economical method for disease control [1].

Constructing a genetic linkage map is a crucial foundation for plant molecular breeding research, as it provides the most direct and rapid access to information about target trait genes and genetic markers. In the genetic map studies of passion fruit, Carneiro et al. [2] and Lopes et al. [3] used 380 RAPD markers and 174 AFLP markers, respectively, to construct genetic maps for yellow passion fruit varieties IAPAR123 and IAPAR06, with both maps containing 9 linkage groups. Later, Oliveira et al. [4] reconstructed an integrated map for yellow passion fruit using 253 AFLP markers and 107 SSR markers, which contained 10 linkage groups. So far, although researchers have developed molecular genetic maps for passion fruit, these maps suffer from low marker density,

 doi:10.20944/preprints202410.2200.v1

limited genome coverage, and low detection efficiency, limiting their application. Therefore, to accelerate the molecular breeding process for disease resistance in cultivated passion fruit, it is essential to construct a high-efficiency, high-density genetic map for the identification of stem rot resistance genes.

The selection of appropriate molecular markers is crucial for constructing a high-density genetic linkage map for cultivated passion fruit. SNP can occur at any location within the genome, and as a new generation of molecular markers, they offer numerous advantages such as high abundance, even distribution, rich polymorphism, and high accuracy [5]. SNP markers have been extensively studied and applied in other plants, but research on their use in passion fruit is only beginning to emerge. da Costa et al. developed 122 primer pairs from 122 transcript sequences of *Passiflora edulis* to amplify the DNA of *Passiflora alata*, and found that there was one SNP every 294 bp [6], whereas in the monocot model plant rice, there is one SNP every 336 bp [7], and in the dicot model plant *Arabidopsis*, one SNP every 333 bp [8]. Nazareno et al. developed 14,536 SNPs in *Passiflora spinosa* using RAD-seq technology and demonstrated, through comparative analysis with the plants *Amphirrhox longifolia* and *Psychotria lupulina*, that rivers act as natural barriers affecting gene flow [9]. Recently, Zheng et al. assembled the genomes of Shaohuang (YPF) and Zihua (PPF), using the passion fruit genome [10] as a reference, and identified 8,069,728 and 7,602,696 SNPs from comparative analysis of YPF and PPF, with an average of 6 SNPs per 1 kb [11]. To date, although researchers have identified a large number of SNPs from the passion fruit genome, there have been no reports of constructing a high-density genetic map using SNP markers for passion fruit.

Stem rot causes severe losses in both the yield and quality of passion fruit, and the types of pathogens vary by region. The reported pathogens causing stem rot in passion fruit mainly include *Fusarium oxysporum*, *Fusarium solani*, and *Phytophthora nicotianae*. In plants such as maize [12-14] and wheat [15-17], researchers have already identified several resistance genes/QTLs. Ye et al. analyzed the function of the QTL *qRfg1* by observing the response of near-isogenic lines of maize infected with *Fusarium graminearum*, and inferred that *qRfg1* encodes a transcription factor that responds to various abiotic stresses [18]. Subsequently, Liu et al. used RNA-seq analysis to reveal that *qRfg1* confers resistance to *Fusarium* stalk rot by constitutively and inducibly expressing defense-related genes, while *qRfg2* enhances maize resistance to stalk rot by relatively low induction of auxin signaling and inhibition of polar auxin transport [19]. Following this, Wang et al. fine-mapped the major QTL *qRfg1* for resistance to *Fusarium graminearum* stalk rot in maize to a 170 kb region, identifying *ZmCCT* as the candidate gene. *ZmCCT* belongs to the CCT gene family, which plays an important role in plant-specific responses to external environmental signals [20]. Recently, Ye et al. fine-mapped the maize QTL *qRfg2* for resistance to *Fusarium graminearum* stalk rot to a 2.6 kb region. The candidate gene *ZmAuxRP1* encodes an auxin-regulated protein that responds rapidly to pathogen attacks, leading to restricted root growth but enhanced resistance to *Fusarium* stalk rot [21]. Zou et al. discovered that the maize cell wall-associated receptor kinase *ZmWAK17* mediates resistance to Fusarium stalk rot [22]. Zhou et al. found that *ZmBT2a* binds with *ZmCUL3* and regulates the transcription of *ZmLOXs* and *ZmPRs* via ubiquitination, thereby contributing to the disease resistance process in maize [23]. Wang et al. evaluated the resistance levels of 435 wheat germplasm resources to stalk rot and identified a novel resistance locus on chromosome 3BL [15]. Yang et al. found that *TaDIR-B1* may regulate wheat's resistance to stem rot by altering lignin content [16]. Lv et al. cloned the gene *TaCWI*, which confers resistance to both wheat stem rot and sheath blight. The gene encodes a cell wall invertase protein that inhibits the expression of the *TaGAL* gene, counteracting its cell wall degradation effect and thickening the cell wall to resist pathogen invasion [17]. Currently, no resistance genes or QTLs for stem rot in passion fruit have been reported domestically or internationally.

In this study, we crossed the passion fruit varieties HG and ZG7 to obtain a BC_1F_1 population, and performed resequencing on the two parents and 158 progenies, constructing a high-density genetic linkage map for passion fruit. Using *Fusarium solani*, we evaluated the resistance of the 158 progenies and identified a resistance locus for stem rot through genetic linkage analysis. This study successfully constructed a high-density genetic linkage map for passion fruit and identified a gene

 doi:10.20944/preprints202410.2200.v1

related to stem rot resistance, which holds significant importance for the breeding of passion fruit varieties resistant to stem rot.

2. Results

2.1. Genome Resequencing

In December 2020 and January 2021, Ma et al. [10] and Xia et al. [32] successfully assembled high-quality reference genomes of passion fruit, with sizes of 1.28 Gb and 1.34 Gb, respectively, each consisting of 9 chromosomes. These genome sequences provide a solid foundation for identifying SNPs using bioinformatics strategies. In this study, the passion fruit genome assembled by Ma et al. [10] was used as the reference for constructing the genetic map.

Sequencing of the two parents, the HG and ZG7, along with 158 BC_1F_1 individuals, was performed using the Illumina NovaSeq 6000 sequencing platform. The raw reads obtained from sequencing contained adapter sequences and low-quality reads. To ensure the data quality, the raw reads were filtered to obtain clean reads for further analysis. The sequencing data for the two parents and the 158 progenies are shown in Table 1.

Table 1. Statistics of sequencing data for ZG7, HG and 158 individuals.

Sample ID	Total Clean Reads (bp)	Total Clean Bases (bp)	Q30 (%)	GC content (%)
ZG7	141877476	41987231840	94.26	42.32
HG	141115213	41852618618	94.39	42.19
Offspring	2939344344	868334262166	93.94	41.95
Total	3222337033	952174112624	93.95	41.96

Using the passion fruit genome as the reference sequence, BWA software was used to realign the clean reads obtained from the resequencing of the two parents and 158 progenies to the reference genome (Table 2). By comparing and locating the position of clean reads on the reference genome, statistics are collected on the sequencing depth, genome coverage and other information of each sample, and mutation detection is performed. The average alignment efficiency for all samples was above 90%, indicating that the sequencing quality was normal.

Table 2. Comparison of ZG7, HG, and 158 individuals to the passion fruit genome.

Sample ID	Clean Reads	Mapped (%)	Properly_mapped (%)
ZG7	283754952	98.63	79.65
HG	282230426	98.75	84.35
Offspring (average)	36970400	98.18	83.02

The reads aligned to the reference genome were analyzed to determine the percentage of sequencing bases that covered the passion fruit genome, and the coverage depth was calculated (Table 3). The average genome coverage depth for the parent samples was over 20×, with genome coverage exceeding 90% (at least 1× coverage). For the progeny samples, the average coverage depth was 3.92×, with coverage exceeding 74.87% (at least 1× coverage).

Table 3. Depth and coverage of sequencing data for ZG7, HG and 158 individuals.

Sample ID	Depth	Coverage ratio 1× (%)	Coverage ratio 5× (%)	Coverage ratio 10× (%)
ZG7	24	99.07	97.35	90.22
HG	28	82.59	74.62	69.03
Offspring (average)	3.92	74.87	31.87	9.14

2.2. SNP Detection

For the results obtained from BWA alignment, Picard's Mark Duplicate toolkit was used to remove PCR duplications. GATK was employed for InDel Realignment, specifically realigning around insertion-deletion regions to correct errors in alignment results caused by InDels. Next, GATK was used for base quality score recalibration (Base Recalibration) to correct base quality values and

 doi:10.20944/preprints202410.2200.v1

detect variants, including SNPs and InDels (1-5 bp). Strict filtering was applied to SNPs and InDels: SNP clusters were filtered if there were 2 SNPs within 5 bp; SNPs near InDels were filtered if there were SNPs within 5 bp of an InDel; and adjacent InDels were filtered (InDels less than 10 bp apart). A total of 5,849,756 SNPs were detected between the two parents, including 4,096,174 transitions and 1,753,582 transversions. ZG7 had 3,566,274 heterozygous SNPs and 2,283,482 homozygous SNPs, while HG had 946,585 heterozygous SNPs and 4,903,171 homozygous SNPs (Table 4). The higher the number of homozygous SNPs, the greater the difference between the sample and the reference genome. Conversely, the higher the number of heterozygous SNPs, the higher the degree of heterozygosity, which relates to the specific characteristics of the selected materials.

Table 4. The decetation of SNPs between ZG7 and HG.

Sample ID	SNP Number	Transition Numbers	Transverison Numbers	Ti/Tv Ratio	Heterozygosity Number	Homozygosity Number
ZG7	5849756	4096174	1753582	2.34	3566274	2283482
HG	5849756	4096174	1753582	2.34	946585	4903171

2.3. Bin Markers

Using the 1,180,406 SNPs obtained, we applied a sliding window approach with 15 SNPs per window and a step size of 1 SNP across the chromosomes. If the number of SNPs with the genotype "aa" within the window was greater than or equal to 13, the window was classified as "aa"; if the number of SNPs with the genotype "bb" was greater than or equal to 13, the window was classified as "bb". In other cases, "ab" was used for genotype imputation and correction. After completing the imputation and correction of markers, Bin segmentation was performed based on the recombination events in the progeny. Ultimately, 4,207 valid Bin markers were obtained on the passion fruit genome.

Using 4,206 Bin markers, a graphical genotype analysis of the 158 progenies was performed (Figure 1). In most lines, there are chromosomes without recombination, entirely derived from a single parental genome. Some chromosome segments in certain lines are heterozygous, which may be due to incomplete or erroneous repair after chromosome crossover.

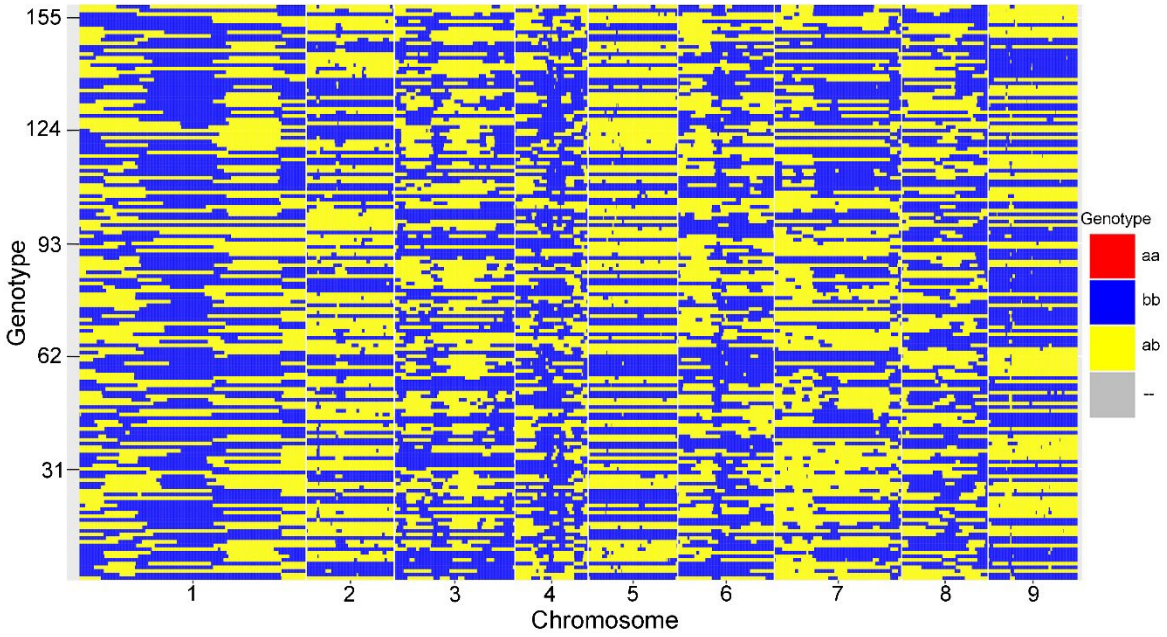

Figure 1. Schematic genotype of passion fruit BC1F1 population. Red segments represent chromosomes derived from the male parent (HG) genome, blue segments represent those from the female parent (ZG7) genome, and orange segments indicate heterozygous regions. The horizontal axis represents chromosome size, while the vertical axis represents the individual progeny numbers.

 doi:10.20944/preprints202410.2200.v1

2.4. Genetic Linkage Map

Using the known information, the Bins were divided into 9 linkage groups. For each linkage group, HighMap software [29] was employed to analyze the linear arrangement of markers and estimate the genetic distance between adjacent markers. The final genetic map covered a total length of 1,559.03 cM (Figure 2).

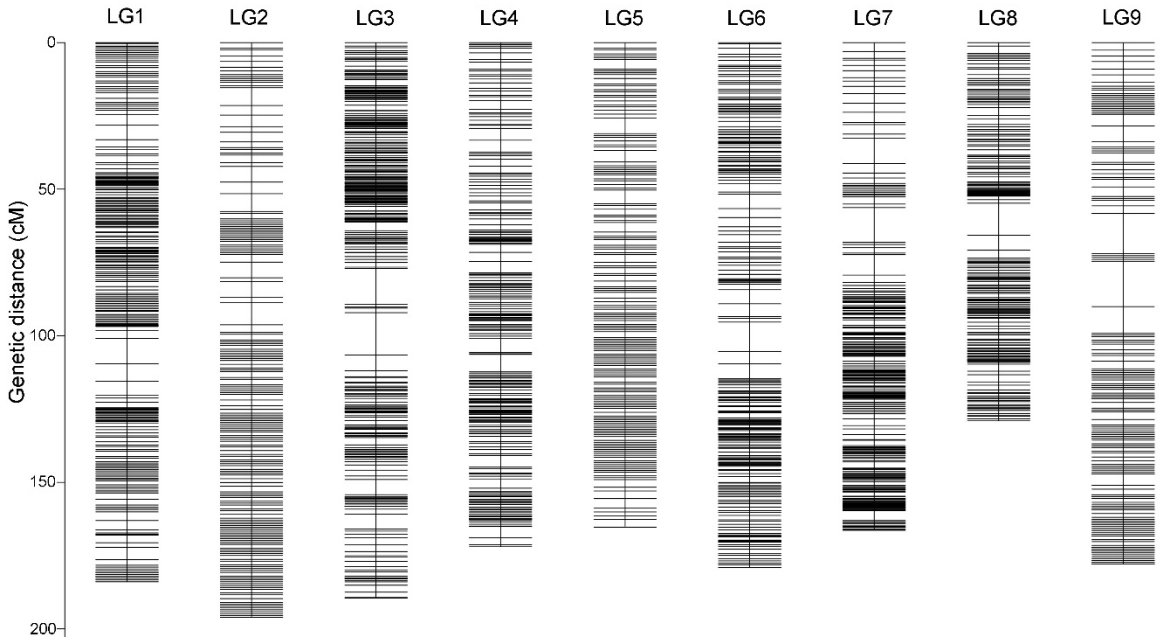

Figure 2. Genetic lengths and marker distribution of 9 linkage groups in genetic map of passion fruit. x-axis represents the linkage groups, y-axis represents the genetic distance.

The 9 linkage groups of cultivated *Passiflora* contained a total of 4,206 Bin markers, ranging from 308 to 956 markers per group. The total genetic distance was 1,559.03 cM, with an average genetic distance of 0.37 cM between Bin markers. The largest gap between markers, 15.45 cM, was located on LG9. Detailed information is presented in Table 5.

Table 5. Statistical analysis of genetic map information of passion fruit.

Linkage group	Total Bin Marker	Total Distance (cM)	Average Distance (cM)	Max Gap (cM)	Gaps<5 cM (%)
LG1	956	183.92	0.19	8.65	98.12%
LG2	371	196.03	0.53	7.5	98.38%
LG3	509	189.5	0.37	14.49	99.02%
LG4	308	171.98	0.56	5.95	99.67%
LG5	378	165.26	0.44	5.34	99.73%
LG6	407	179.08	0.44	10.01	99.51%
LG7	537	166.35	0.31	11.9	99.44%
LG8	364	129.04	0.36	10.91	99.45%
LG9	376	177.87	0.47	15.45	98.93%
Total	4206	1559.03	0.37	15.45	98.12%

2.5. Linkage Assessment and Collinearity Analysis

The genetic map is essentially a result of multipoint recombination analysis, where the smaller the genetic distance between markers, the lower the recombination rate. By analyzing the recombination relationships between markers and their neighboring markers, potential mapping errors or problematic markers can be identified. Figure 3 presents the recombination heatmap of the markers, showing the linkage relationships across all linkage groups.

 doi:10.20944/preprints202410.2200.v1

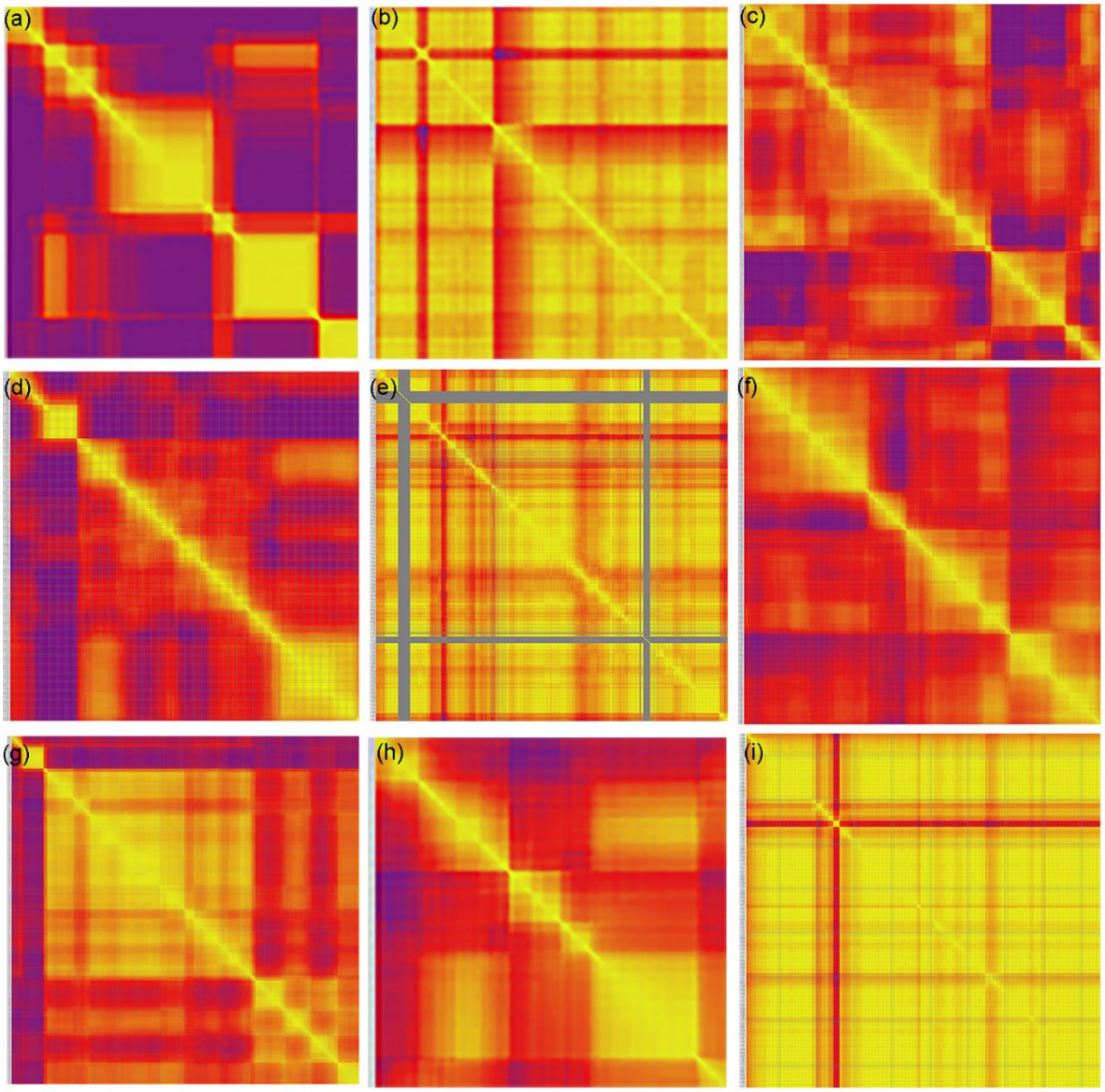

Figure 3. Marker linkage relationship diagram of nine linkage groups in passion fruit. Each row and column are arranged in the order of the graph as markers, with each small square representing the recombination rate between two markers. The change in color from yellow to red to purple represents the variation in recombination rate from small to large. The closer the distance, the lower the recombination rate of the marker, and the closer the color is to yellow. The farther the distance, the higher the recombination rate of the marker, and the closer it is to purple.

Next, a collinearity analysis was performed by using the position of the markers on the genome and the genetic map. This analysis helps to assess the accuracy of the genetic map compared to the reference genome. The collinearity between the genetic map and the physical genome is depicted in the figure below. To further quantify the relationship between each linkage group, Spearman's correlation coefficient was calculated for each linkage group. The closer the Spearman coefficient is to 1, the better the collinearity between the genetic map and the physical genome. The Spearman correlation for each linkage group with the reference genome is shown in Figure 4.

 doi:10.20944/preprints202410.2200.v1

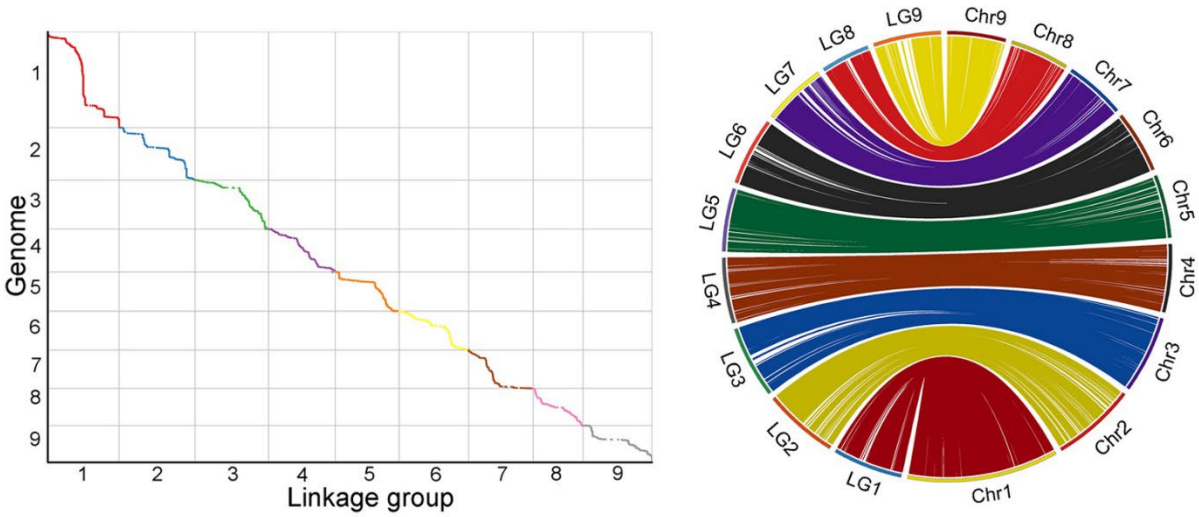

Figure 4. Collinearity between genetic and reference genome in passion fruit. (a) The relationship between linkage groups and genomes. (b) Visualization of collinearity. x-axis represents genetic distance, y-axis represents physical distance.

2.6. Analysis of Passion Fruit Stem Rot

The identification results showed that the incidence rates of HG and ZG7 were 29.7% and 81.2%, respectively. The incidence rate of stem rot in BC_1F_1 population are continuously distributed, showing a quantitative genetic model (Figure 5). The minimum incidence rate in 158 individuals was 25.4%, and the maximum was 81.2%. The difference is significant.

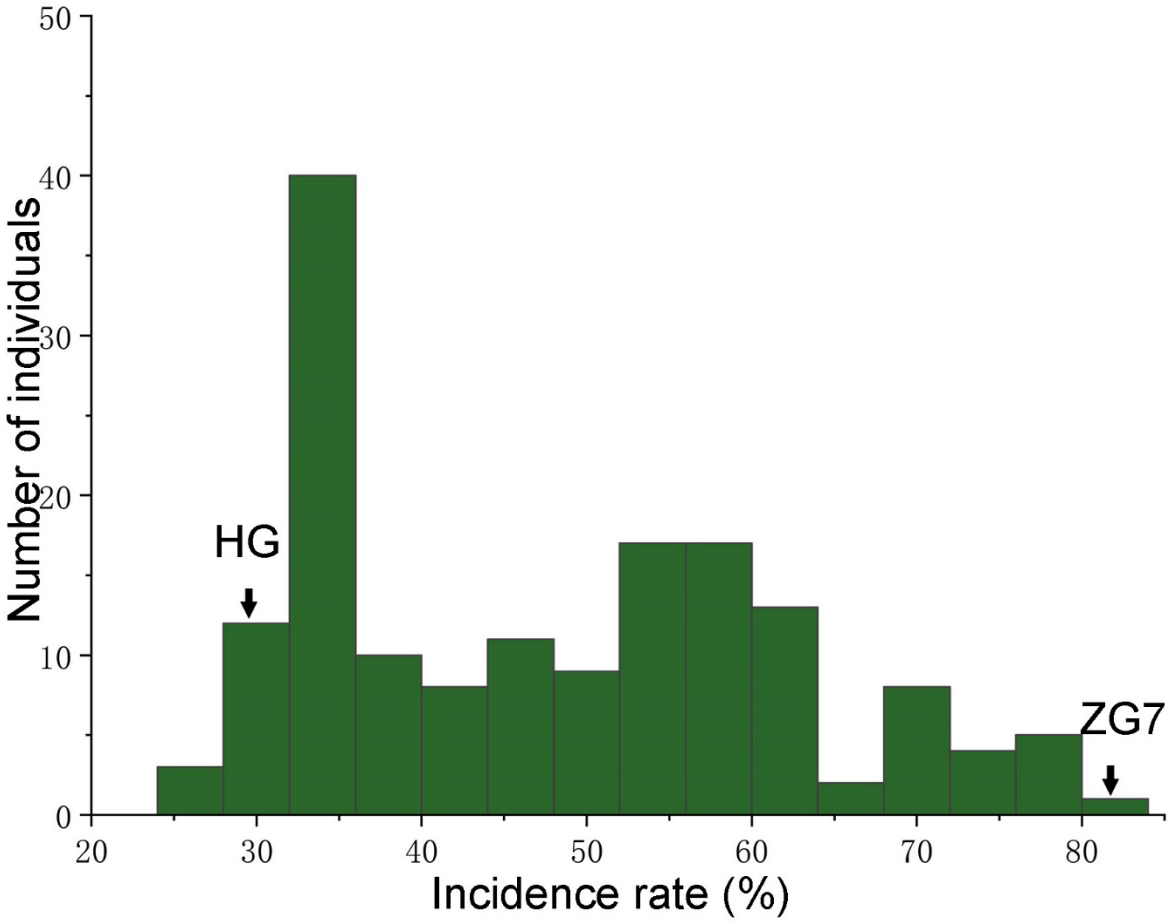

 doi:10.20944/preprints202410.2200.v1

Figure 5. Distribution of stem rot disease resistance in the passion fruit BC_1F_1 population. The x-axis shows the ranges of phenotypic traits and the y-axis represents the number of individuals in the BC_1F_1 population.

2.7. Mapping of Resistance Loci for Stem Rot and Analysis of Candidate Genes

The MapQTL interval mapping method was used to locate the trait, and the threshold was set by 1000 PT tests. A total of one QTL was detected for passion fruit stem rot resistance, located at 145.878-152.951 cM on linkage group 5, with a contribution rate of 8.6% (Figure 6). Subsequently, we named this gene the *quantitative trait locus for passion fruit stem rot disease resistance on chromosome 5* (*qPSR5*).

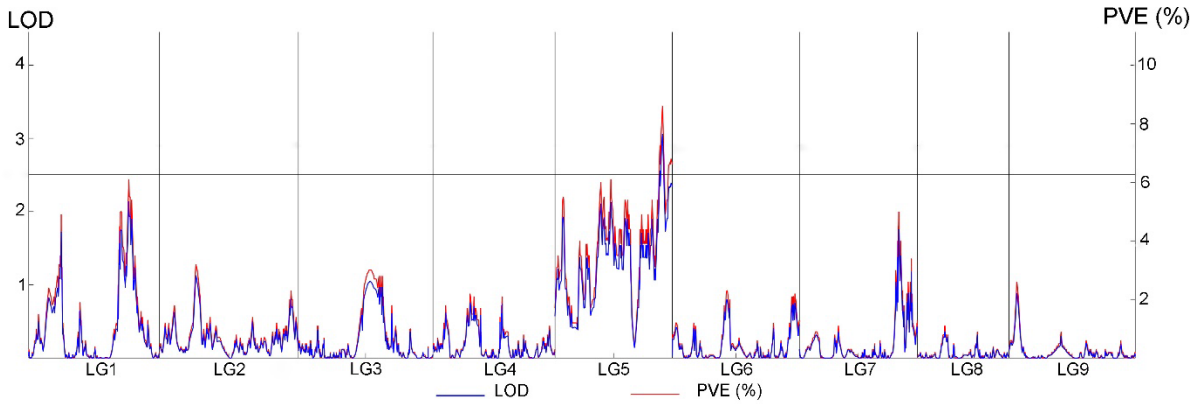

Figure 6. QTL mapping for stem rot disease resistance on linkage group 5 in the passion fruit. The x-axis represents the linkage groups, LOD: the logarithm of odds score, PVE: the percentage of the phenotypic variance explained by individual QTL.

Based on the analysis results, we aligned the bin markers to the passion fruit genome within the 113,377,860 bp-114,811,870 bp region, which contains 33 candidate genes (Supplementary Table 2). Among them, *ZX.05G0020700*, *ZX.05G0020740*, *ZX.05G0020790*, and *ZX.05G0020880* encode NAC domain proteins. Previous studies have shown that NAC transcription factors enhance plant responses to biotic stress by regulating the expression of disease resistance-related genes [33-36]. *ZX.05G0020810* is also associated with increased disease resistance, encoding a zinc ribbon domain-containing protein. In the previous studies, we used RNA-seq to identify differentially expressed genes (DEGs) in response to *Fusarium solani* infection in both HG and ZG7, identifying a total of 6,801 DEGs[37] (Supplementary Table 3). Within the candidate region for the stem rot resistance gene *qPSR5*, there are 5 DEGs (Table 6). One of these, *ZX.05G0020920*, encodes a WAT1-related protein, and the *WAT1* gene (*At01g75500*) in *Arabidopsis* has been shown to mediate resistance to pathogens [38,39] (Table 6).

Table 6. Candidate genes and annotation information for the stem rot disease resistance in passion fruit.

Gene	Annotation
ZX.05G0020700	NAC domain-containing protein 14
ZX.05G0020740	NAC domain-containing protein 91
ZX.05G0020760	DNA/RNA polymerases superfamily protein
ZX.05G0020810	Protein ENHANCED DISEASE RESISTANCE 4
ZX.05G0020830	B3 domain-containing transcription factor
ZX.05G0020920	WAT1-related protein

Using *EF1* as a reference gene, we performed RT-qPCR to detect the expression levels of *ZX.05G0020700*, *ZX.05G0020740*, *ZX.05G0020760*, *ZX.05G0020830*, *ZX.05G0020920*, and *ZX.05G0020810* in both HG and ZG7 (Figure 7). The results indicated that the expression levels of

 doi:10.20944/preprints202410.2200.v1

ZX.05G0020740 and *ZX.05G0020810* were significantly different in HG and ZG7, while the expression level of *ZX.05G0020700* was no significance.

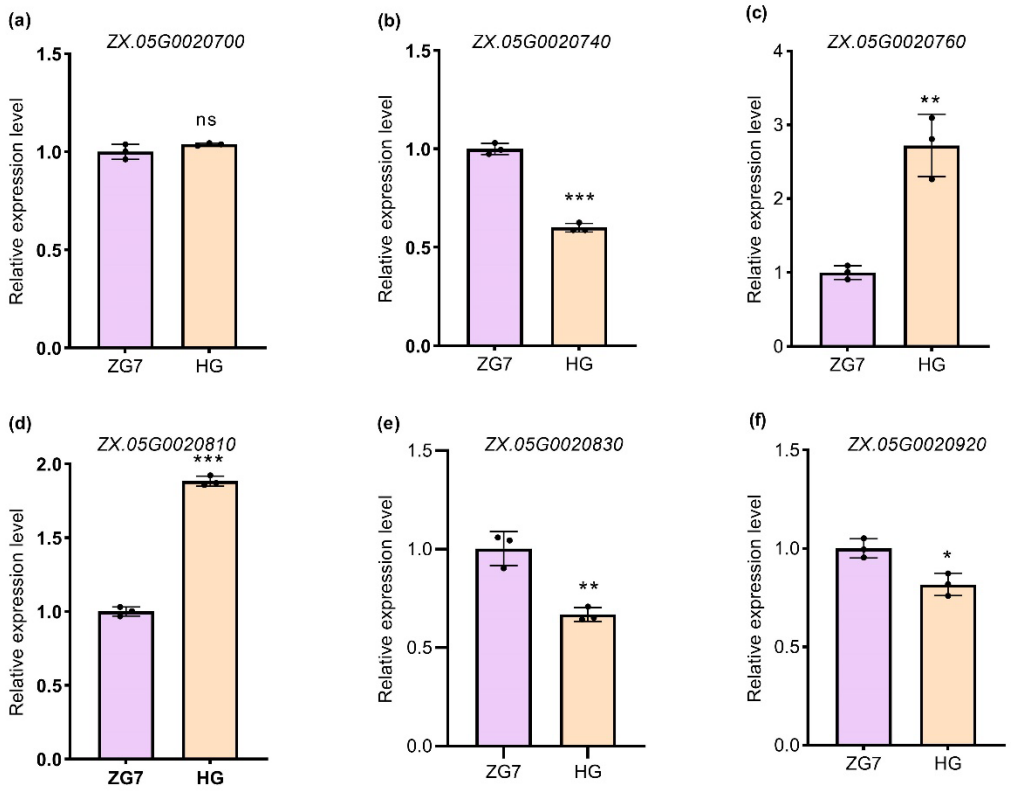

Figure 7. Relative expression of candidate genes between HG and ZG7. Data are represented as mean ± SD. *$P < 0.05$, **$P < 0.01$, ***$P < 0.0001$, ns indicates no significance, siwith Student's *t*-test.

3. Discussion

A genetic linkage map is a linear diagram that shows the order and relative distances between different genes or specific polymorphic markers on the same chromosome. Constructing a genetic map requires an appropriate population, with commonly used mapping populations including F_1, F_2, BC, RILs, and DH. Although yellow passion fruit has strong resistance to stem rot disease, it exhibits self-incompatibility [40]. Since the choice of parents directly determines the quality of the genetic map and its applicability in future research, to construct a high-quality genetic map for cultivated passion fruit, we crossed ZG7 as the maternal parent with HG as the paternal parent to obtain an F_1 population, and then backcrossed ZG7 to generate the BC_1F_1 population. Studies have shown that the appropriate population size for constructing a genetic map ranges from 100 to 300 individuals [41-43]. In this study, we used 158 BC_1F_1 passion fruit individuals to construct the genetic map, which falls within the reasonable size range.

In the study of constructing high-density genetic maps using SNPs, although highly refined genome maps have already been assembled for crops like rice and Arabidopsis, high-density SNP genetic maps remain essential tools for gene mapping research in these species [44,45]. In research on other species, Zhou et al. used GBS technology to sequence a maize recombinant inbred line (RILs, F_{11}) population and constructed a high-density genetic map with 88,268 SNPs, successfully locating plant architecture-related genes and predicting the *qPH10* gene [46]. Sun et al. used RAD-seq technology to sequence an F_1 population of apples, selecting 3,441 high-quality SNP markers to construct a high-density genetic map of apples and successfully mapped three QTLs for quality traits [47]. Yu et al. constructed a genetic map for broccoli using a double haploid (DH) population containing 9,367 SNPs and identified a locus, *QHS.C09-2*, associated with the hollow stem trait [48]. Shirasawa et al. successfully constructed a high-density genetic linkage map for hexaploid sweet

 doi:10.20944/preprints202410.2200.v1

potato using SNP markers, providing valuable reference data for constructing genetic maps in other polyploid plants [49]. These studies demonstrate that SNP markers, as an efficient and practical molecular marker, can be used to construct high-density genetic maps and locate target trait genes or QTLs across model and non-model species, monocots and dicots, diploid and polyploid plants, and both temporary and permanent mapping populations. In this study, we utilized resequencing technology to sequence the passion fruit varieties HG and ZG7, as well as their BC_1F_1 population, and constructed a high-density genetic map for passion fruit. The map includes 9 linkage groups with a total genetic distance of 1,559.03 cM and an average genetic distance of 0.404 cM between each bin marker, showing significantly higher resolution compared to the genetic maps constructed by Carneiro et al. [2], Lopes et al. [3], and Oliveira et al. [4]. Additionally, the high-density SNP marker genetic map showed a collinearity correlation coefficient of 0.9994 with the passion fruit genome, indicating the high quality of the map.

In my previous research, we found that genes related to reactive oxygen species (ROS), lignin biosynthesis, and leucine-rich repeat domain proteins play a crucial role in passion fruit resistance to stem rot disease [37]. In this study, through genetic linkage analysis, RNA-seq, and RT-qPCR, we identified that *ZX.05G0020700*, *ZX.05G0020740*, and *ZX.05G0020920* are likely involved in regulating resistance to passion fruit stem rot disease. Both *ZX.05G0020700* and *ZX.05G0020740* are NAC transcription factors. NAC transcription factors in plants not only regulate the growth of secondary cell walls [50-53] but also participate in responses to biotic and abiotic stresses [54]. Research has shown that lignin biosynthesis plays a diversified role in plant disease resistance [55,56], with NAC transcription factors regulating this process. For example, in rice, OsNAC5 can directly activate the expression of *OsCCR10*, which is involved in the biosynthesis of H- and G-lignin, thereby regulating drought tolerance by controlling lignin accumulation [57]. OsNAC028 is involved in lignin synthesis and positively regulates resistance to rice sheath blight [58]. OsNAC29/31 are top-tier transcription factors controlling secondary wall formation and activating Os*MYB61*, which in turn stimulates the expression of secondary wall cellulose synthesis genes [59]. OsNAC045 reduces stress-induced root growth inhibition by enhancing lignin synthesis in roots and reducing ROS accumulation in response to cold and salt stresses [60]. In wheat, TaNAC032 regulates lignin biosynthesis and enhances resistance to *Fusarium* head blight [34]. NAC transcription factors also regulate disease resistance genes, enhancing plant immunity. For instance, OsMNAC3 activates negative immune regulators such as *OsINO80*, *OsJAZ10*, and *OsJAZ11*, which negatively regulate resistance to rice blast and bacterial blight [36]. ONAC122 and ONAC131 play critical roles in disease resistance in rice by regulating the expression of defense-related and signaling genes [61]. ONAC083 activates OsRFPH2-6, negatively regulating rice immunity to blast fungus [62]. Despite *OsNAC60* overexpression enhancing defense responses, it negatively regulates rice immunity to blast [63]. In barley, the NAC transcription factor Rph7 mediates resistance to rust [35], while in wheat, TaNAC30 negatively regulates resistance to stripe rust [64]. The passion fruit genome contains 105 NAC transcription factors. After *Fusarium kyushuense* infection, 15 *NAC* genes showed significantly different expression levels in yellow and purple passion fruit, with *PeNAC001*, *PeNAC003*, *PeNAC028*, *PeNAC033*, *PeNAC057*, *PeNAC058*, *PeNAC063*, and *PeNAC077* suspected to play key roles in *Fusarium kyushuense* resistance [65]. In this study, *ZX.05G0020700* (*PeNAC068*) and *ZX.05G0020740* (*PeNAC069*) exhibited significant expression changes after *Fusarium solani* infection in HG and ZG7, suggesting these genes may play important roles in passion fruit resistance to stem rot disease.

WAT1 (*Walls Are Thin 1*) is an Arabidopsis homolog of Medicago truncatula *NODULIN21*, essential for secondary wall formation in fibers [66]. The secondary cell wall (SCW) is a critical part of the plant cell wall, located inside the primary wall and gradually formed and thickened during cell growth and development. SCWs are composed primarily of complex polymers like cellulose, lignin, and hemicellulose. These components and structures provide SCWs with many important functions, such as mechanical support, water and nutrient transport, and resistance against pathogen invasion [67]. Denancé found that *Arabidopsis* wat1 (walls are thin1) mediates resistance to the bacterial vascular pathogen *Ralstonia solanacearum* [38]. Koseoglou et al. showed that inactivation of *WAT1* in tomato reduced susceptibility to *Clavibacter michiganensis* by downregulating bacterial virulence

 doi:10.20944/preprints202410.2200.v1

factors [68]. In this study, significant differences in *NAC* and *WAT1* gene expression were observed between HG and ZG7, and previous research has demonstrated that NAC transcription factors regulate the growth of plant secondary cell walls [50-53]. Therefore, it is likely that NAC transcription factors and *WAT1* genes jointly contribute to the regulation of passion fruit stem rot disease resistance.

4. Materials and Methods

4.1. Plant Materials

F_1 generation was obtained by crossbreeding Ziguo7 (ZG7, female parent) and Huangguoyuanshengzhong (HG, male parent). Then use F_1 generation to hybridize with ZG7 to obtain BC_1F_1 population. The experimental materials, HG, ZG7, and 158 progenies, were planted at the Meilinanfang of Guangxi Academy of Agricultural Sciences. Stem rot samples were collected from the boundary between healthy and infected tissue at the stem of passion fruit plants, and the pathogen was isolated and placed on potato dextrose agar (PDA) medium, primarily identified as *Fusarium solani*. To assess the disease resistance of the passion fruit plants, we used an *in vitro* inoculation method. The purified and preserved pathogen was reactivated and cultured on PDA medium at 28°C for 5 days. Mycelial plugs were obtained using a 1000 μL sterilized pipette tip. For the disease resistance evaluation, an artificial wound was made at the stem, and the prepared mycelial plugs were placed on the wound, with the mycelium facing directly against the wound site. Each progeny family was planted with 15 plants, and the disease incidence rate was recorded.

4.2. DNA Extraction

At the 6-8 leaf stage, young leaves from the two parents and 158 individuals were collected and stored at -80 °C. Genomic DNA from the parents and BC_1F_1 population was extracted using the CTAB method. The DNA concentration was measured with a Qubit 2.0 Fluorometer, and the purity and integrity of the DNA were assessed using 1% agarose gel electrophoresis.

4.3. Resequencing and SNP Calling

After the DNA samples passed quality control, the DNA was randomly fragmented using ultrasonication. The DNA fragments were then subjected to end repair, 3' end A-tailing, sequencing adapter ligation, purification, and PCR amplification to construct the sequencing library. Once the library passed quality control, sequencing was performed on the Illumina NovaSeq 6000 platform.

The raw sequencing data were assessed and filtered for quality using Cutadapt software[24] and Trimmomatic software[25]. The main steps for data filtering were as follows: (1) removing adapter sequences; (2) filtering out paired-end reads where the proportion of 'N' bases (undetermined nucleotides) was greater than 10%; and (3) removing low-quality reads, where more than 50% of the bases in the read had a quality score of $Q \leq 10$.

Using the passion fruit genome as a reference, we employed BWA software [26] to align the clean reads to the reference genome, generating SAM format alignment results. SAMtools software (version 1.3.1) was then used to convert the SAM files into BAM format. Subsequently, the Picard tool (version 1.91) (http://sourceforge.net/projects/picard/) was used to sort the reads in the BAM files using the SortSam function. The final BAM files were utilized for coverage and depth statistics, as well as for variant calling. Next, the HaplotypeCaller module from the GATK (version 3.7) software package [27] was used to generate gvcf files for each sample, followed by SNP detection across all samples using the GenotypeGVCFs module.

4.4. Genetic Maping

Based on the resequencing results, SNP genotyping and filtering were performed on the parents and 158 RILs. Following the method published by Huang et al., a sliding window approach was used, where each window contained 15 SNPs, and the step size was 1 SNP along the chromosome. If 13 or more SNPs in the window were genotyped as "aa", the window was classified as "aa". Similarly, if 13 or more SNPs were genotyped as "bb," the window was classified as "bb." In other cases, the genotype

 doi:10.20944/preprints202410.2200.v1

was filled and corrected as "ab" [28]. Afterward, the HighMap software[29] was used for linkage grouping, marker ordering, genotype correction, and map evaluation.

4.5. QTL Analysis

Trait mapping was performed using the interval mapping method in MapQTL 6 (https://www.kyazma.nl/index.php/MapQTL/Updates/), and a permutation test (PT) was conducted 1000 times to set the threshold value. The IM algorithm in the MapQTL software were used for QTL mapping. When the LOD score at a certain position exceeded the threshold, we would consider a QTL present at that location. At a 5% significance level, a critical value of 2.5 was used, meaning that an LOD score of ≥2.5 was taken as the threshold for determining the existence of a QTL.

4.6. Candidate Gene Analysis

Using the physical position corresponding to the mapped interval, the candidate genes were screened through the annotation function of the passion fruit genome database, combined with the results from previous RNA-seq analyses[30].

4.7. RT-qPCR

Total RNA was extracted using the TRIzol® Reagent kit (Invitrogen, USA), following the manufacturer's instructions. *EF1* was used as the reference gene[31], and RT-qPCR was employed to validate the candidate genes and primers listed in Supplementary Table 1. The detailed RT-qPCR procedure followed the methods described in a previously published paper [30].

4.8. Statistical Analysis

Origin2019B software was used for statistical analysis. CorelDRAW X8 software was utilized for data visualization and figure generation. Primers were designed using Primer 5 software.

5. Conclusions

In this study, we utilized SNP markers to construct the first high-density genetic linkage map for cultivated passion fruit. This map consists of 9 linkage groups, with a total genetic distance of 1559.03 cM, an average genetic distance of 311.806 cM, and an average distance between 4206 bins of 0.404 cM, with a mean gap length of 10.565 cM. The collinearity correlation coefficient between the genetic map and the genome of *Passiflora edulis* was 0.9994. Using this genetic map, we identified one locus for stem rot disease resistance on linkage group 5, located between 145.878 cM and 152.951 cM, contributing 8.6% to the resistance. Through RNA-seq and RT-qPCR analysis, we detected the expression levels of predicted genes within the candidate region, identifying *ZX.05G0020740 and ZX.05G0020810* as ideal candidate genes for resistance to stem rot disease in passion fruit. The construction of this high-efficiency, high-density genetic map provides a strong foundation for identifying QTLs related to stem rot disease resistance and closely linked molecular markers, laying the groundwork for the genetic improvement and molecular breeding of cultivated passion fruit.

Author Contributions: Conceptualization, X.Y. and H.M.; methodology, Y.W. and J.L.; formal analysis, Y.W. and J.Z.; validation, J.Z., Q.T. and Y.W.; investigation, W.H., X.X. and Q.T.; writing—original draft preparation, Y.W.; writing—review and editing, X.Y. and H.M.; supervision, H.M. All authors have read and agreed to the published version of the manuscript.

Funding: This work was supported by the National Natural Science Foundation of China (No.32060660 and 32260740), Guangxi Natural Science Foundation of China (2023GXNSFAA026301), Guangxi Ministry of Science and Technology (GuikeAA22068091-1), Guangxi Academy of Agricultural Sciences (2021YT089).

Conflicts of Interest: The authors declare no conflicts of interest.

Data Availability Statement: The RNA-seq data that support the findings of this study have been deposited to National Center for Biotechnology Information (NCBI) Sequence Read Archive (SRA) with the accession code PRJNA1102446 (SRA no. from SRR28748077 to SRR28748094).

 doi:10.20944/preprints202410.2200.v1

References

1. Nelson R, Wiesner-hanks T, Wisser R, Balint-kurti P. Navigating complexity to breed disease-resistant crops. Nat Rev Genet, 2018, 19(1): 21-33.
2. Carneiro MS, Camargo LE, Coelho AS, Vencovsky R, Rui PL, Stenzel NM, Vieira ML. RAPD-based genetic linkage maps of yellow Passion fruit (Passiflora edulis Sims. f. flavicarpa Deg.). Genome, 2002, 45(4): 670-678.
3. Lopes R, Lopes MT, Carneiro MS, Matta FP, Camargo LE, Vieira ML. Linkage and mapping of resistance genes to Xanthomonas axonopodis pv. passiflorae in yellow Passion fruit. Genome, 2006, 49(1): 17-29.
4. Oliveira EJ, Vieira M, Garcia A, Munhoz CF, Margarido G, Consoli L, Matta FP, Moraes MC, Zucchi MI, Fungaro M. An integrated molecular map of yellow Passion fruit based on simultaneous Maximum-likelihood estimation of linkage and linkage phases. J Am Soc Hortic Sci, 2008, 133(1): 35-41.
5. Ganal W, Altmann T, Röder MS. SNP identification in crop plants. Curr Opin Plant Biol, 2009, 12: 211-217.
6. Costa ZD, Munhoz CF, Vieira M. Report on the development of putative functional SSR and SNP markers in Passion fruits. BMC Res Notes, 2017, 10(1): 445.
7. Schmid K, Sorensen TR, Stracke R, Torjek O, Altmann T, Mitchell-olds T, Weisshaar B. Large-scale identification and analysis of genome-wide single-nucleotide polymorphisms for mapping in Arabidopsis thaliana. Genome Res, 2003, 13(6): 1250-1257.
8. Yu J, Wang J, Lin W, Li S, Li H, Zhou J, Ni P, Dong W, Hu S, Zeng C, Zhang J, Zhang Y, Li R, Xu Z, Li S, Li X, Zheng H, Cong L, Lin L, Yin J, Geng J, Li G. The genomes of oryza sativa: a history of duplications. PLoS Biol, 2005, 3(2): e38.
9. Nazareno AG, Dick CW, Lohmann LG. Tangled banks: a landscape genomic evaluation of wallace's riverine barrier hypothesis for three Amazon plant species. Mol Ecol, 2018, 28(5): 980-997.
10. Ma D, Dong S, Zhang S, Wei X, Xie Q, Ding Q, Xia R, Zhang X. Chromosome-level reference genome assembly provides insights into aroma biosynthesis in Passion fruit (Passiflora edulis). Mol Ecol Resour, 2021, 21(3): 955-968.
11. Zheng YY, Chen LH, Fan BL, Xu Z, Wang Q, Zhao BY, Gao M, Yuan MH, Tahir UM, Jiang Y, Yang L, Wang L, Li W, Cai W, Ma C, Lu L, Song JM, Chen LL. Integrative multiomics profiling of Passion fruit reveals the genetic basis for fruit color and aroma. Plant Physiol, 2024, 194(4): 2491-2510.
12. Ma C, Ma X, Yao L, Liu Y, Du F, Yang X, Xu M. qRfg3, a novel quantitative resistance locus against gibberella stalk ROT in maize. Theor Appl Genet, 2017, 130(8): 1723-1734.
13. Duan C, Song F, Sun S, Guo C, Zhu Z, Wang X. Characterization and molecular mapping of two novel genes resistant to Pythium stalk rot in maize. Phytopathology, 2019, 109(5): 804-809.
14. Chen Q, Song J, Du WP, Xu LY, Jiang Y, Zhang J, Xiang XL, Yu GR. Identification, mapping, and molecular marker development for Rgsr8.1: a new quantitative trait locus conferring resistance to Gibberella stalk rot in maize (Zea mays L.). Front Plant Sci, 2017, 8: 1355.
15. Wang C, Sun M, Zhang P, Ren X, Zhao S, Li M, Ren Z, Yuan M, Ma L, Liu Z, Wang K, Chen F, Li Z, Wang X. Genome-wide association studies on Chinese wheat cultivars reveal a novel Fusarium crown rot resistance quantitative trait locus on chromosome 3BL. Plants, 2024, 13(6): 856.
16. Yang X, Zhong S, Zhang Q, Ren Y, Sun C, Chen F. A loss-of-function of the dirigent gene TaDIR-B1 improves resistance to Fusarium crown rot in wheat. Plant Biotechnol J, 2021, 19(5): 866-868.
17. Lv G, Zhang Y, Ma L, Yan X, Yuan M, Chen J, Cheng Y, Yang X, Qiao Q, Zhang L, Niaz M, Sun X, Zhang Q, Zhong S, Chen F. A cell wall invertase modulates resistance to fusarium crown rot and sharp eyespot in common wheat. J Integr Plant Biol, 2023, 65(7): 1814-1825.
18. Ye J, Guo Y, Zhang D, Zhang N, Wang C, Xu M. Cytological and molecular characterization of quantitative trait locus qRfg1, which confers resistance to Gibberella stalk rot in maize. Mol Plant Microbe Interact, 2013, 26(12): 1417-1428.
19. Liu Y, Guo Y, Ma C, Zhang D, Wang C, Yang Q. Transcriptome analysis of maize resistance to Fusarium graminearum. BMC Genomics, 2016, 17: 477.
20. Wang C, Yang Q, Wang W, Li Y, Guo Y, Zhang D, Ma X, Song W, Zhao J, Xu M. A transposon-directed epigenetic change in ZmCCT underlies quantitative resistance to Gibberella stalk rot in maize. New Phytol, 2017, 215(4): 1503-1515.
21. Ye J, Zhong T, Zhang D, Ma C, Wang L, Yao L, Zhang Q, Zhu M, Xu M. The auxin-regulated protein ZmAuxRP1 coordinates the balance between root growth and stalk rot disease resistance in maize. Mol Plant, 2019, 12(3): 360-373.
22. Zuo N, Bai WZ, Wei WQ, Yuan TL, Zhang D, Wang YZ, Tang WH. Fungal CFEM effectors negatively regulate a maize wall-associated kinase by interacting with its alternatively-spliced variant to dampen resistance. Cell Rep, 2022, 41(13): 111877.
23. Zhou F, Wang Y, Liu P, Ma W, He R, Cao H, Xing J, Zhang K, Dong J. Function of ZmBT2a gene in resistance to pathogen infection in maize. Phytopathol Res, 2024, 6: 43.
24. Martin M. CUTADAPT removes adapter sequences from high-throughput sequencing reads. EMBnet J, 2011, 17: 10-12.

25. Bolger AM, Lohse M, Usadel B. Trimmomatic: a flexible trimmer for Illumina sequence data. Bioinformatics, 2014, 30(15): 2114-2120.
26. Li H, Durbin R. Fast and accurate short read alignment with Burrows-Wheeler transform. Bioinformatics, 2009, 25(14): 1754-1760.
27. Mckenna A, Hanna M, Banks E, Sivachenko A, Cibulskis K, Kernytsky A, Garimella K, Altshuler D, Gabriel S, Daly M, Depristo MA. The genome analysis toolkit: a MapReduce framework for analyzing next-generation DNA sequencing data. Genome Res, 2010, 20(9): 1297-1303.
28. Huang X, Feng Q, Qian Q. High-throughput genotyping by whole-genome resequencing. Genome Res, 2009, 19(6): 1068-1076.
29. Liu D, Ma C, Hong W, Huang L, Liu M, Liu H, Zeng H, Deng D, Xin H, Song J, Xu C, Sun X, Hou X, Wang X, Zheng H. Construction and analysis of high-density linkage map using high-throughput sequencing data. PLoS One, 2014, 9(6): e98855.
30. Wu Y, Huang W, Tian Q, Liu J, Xia X, Yang X, Mou H. Comparative transcriptomic analysis reveals the cold acclimation during chilling stress in sensitive and resistant Passion fruit (Passiflora edulis) cultivars. PeerJ, 2021, 9: e10977.
31. Zhao M, Fan H, Tu Z, Cai G, Zhang L, Li A, Xu M. Stable reference gene selection for quantitative real-time PCR normalization in Passion fruit (Passiflora edulis Sims.). Mol Biol Rep, 2022, 49(7): 5985-5995.
32. Xia Z, Huang D, Zhang S, Wang W, Ma F, Wu B, Xu Y, Xu B, Chen D, Zou M, Xu H, Zhou X, Zhan R, Song S. Chromosome-scale genome assembly provides insights into the evolution and flavor synthesis of Passion fruit (Passiflora edulis Sims). Hortic Res, 2021, 8(1): 14.
33. Liu Q, Yan S, Huang W, Yang J, Dong J, Zhang S, Zhao J, Yang T, Mao X, Zhu X, Liu B. NAC transcription factor ONAC066 positively regulates disease resistance by suppressing the ABA signaling pathway in rice. Plant Mol Biol, 2018, 98(4/5): 289-302.
34. Soni N, Altartouri B, Hegde N, Duggavathi R, Nazarian-firouzabadi F, Kushalappa AC. TaNAC032 transcription factor regulates lignin-biosynthetic genes to combat Fusarium head blight in wheat. Plant Sci, 2021, 304: 110820.
35. Chen C, Jost M, Outram MA, Friendship D, Chen J, Wang A, Periyannan S, Bartoš J, Holušová K, Doležel J, Zhang P, Bhatt D, Singh D, Lagudah E, Park RF, Dracatos PM. A pathogen-induced putative NAC transcription factor mediates leaf rust resistance in barley. Nat Commun, 2023, 14(1): 5468.
36. Wang H, Bi Y, Yan Y, Yuan X, Gao Y, Noman M, Li D, Song F. A NAC transcription factor MNAC3-centered regulatory network negatively modulates rice immunity against blast disease. J Integr Plant Biol, 2024: Jul 2.
37. Wu Y, Shi G, Zhou J, Tian Q, Liu J, Huang W, Xia X, Mou H, Yang X. Identification and validation of stem rot disease resistance genes in Passion fruit (Passiflora edulis). Hortic Sci, 2025, 52(1): 1-22.
38. Denancé N, Ranocha P, Oria N, Barlet X, Rivière MP, Yadeta KA, Hoffmann L, Perreau F, Clément G, Maia-grondard A, Van den berg GC, Savelli B, Fournier S, Aubert Y, Pelletier S, Thomma BP, Molina A, Jouanin L, Marco Y, Goffner D. Arabidopsis wat1 (walls are thin1)-mediated resistance to the bacterial vascular pathogen, Ralstonia solanacearum, is accompanied by cross-regulation of salicylic acid and tryptophan metabolism. Plant J, 2013, 73(2): 225-239.
39. Hanika K, Schipper D, Chinnappa S, Oortwijn M, Schouten HJ, Thomma B, Bai Y. Impairment of tomato WAT1 Enhances resistance to Vascular wilt fungi despite severe growth defects. Front Plant Sci, 2021, 12: 721674.
40. Rêgo MM, Rêgo ER, Bruckner CH, Silva EA, Finger FL, Pereira KC. Pollen tube behavior in yellow Passion fruit following compatible and incompatible crosses. Theor Appl Genet, 2000, 101(5/6): 685-689.
41. Zhang W, Lu Z, Guo T, Yuan C, Liu J. Construction of a high-density genetic map and QTL localization of body weight and wool production related traits in Alpine Merino sheep based on WGR. BMC Genomics, 2024, 25(1): 641.
42. Zhang Z, Xie W, Zhang J, Wang N, Zhao Y, Wang Y, Bai S. Construction of the first high-density genetic linkage map and identification of seed yield-related QTLs and candidate genes in Elymus sibiricus, an important forage grass in Qinghai-Tibet Plateau. BMC Genomics, 2019, 20(1): 861.
43. Wang X, Chen Z, Li Q, Zhang J, Liu S, Duan D. High-density SNP-based QTL mapping and candidate gene screening for yield-related blade length and width in Saccharina japonica (Laminariales, Phaeophyta). Sci Rep, 2018, 8(1): 13591.
44. Neelam K, Mahajan R, Gupta V, Bhatia D, Gill BK, Komal R, Lore JS, Mangat GS, Singh K. High-resolution genetic mapping of a novel bacterial blight resistance gene xa-45(t) identified from Oryza glaberrima and transferred to Oryza sativa. Theor Appl Genet, 2019: 页码范围缺失.
45. Ear S, Snoek LB, Nijveen H, Laj W, Jiménez-gómez JM, Hilhorst H, Ligterink W. Construction of a High-Density genetic map from RNA-Seq data for an arabidopsis Bay-0 × shahdara RIL population. Front Genet, 2017, 8: 201.

 doi:10.20944/preprints202410.2200.v1

46. Zhou Z, Zhang C, Zhou Y, Hao Z, Wang Z, Zeng X, Di H, Li M, Zhang D, Yong H, Zhang S, Weng J, Li X. Genetic dissection of maize plant architecture with an ultra-high density bin map based on recombinant inbred lines. BMC Genomics, 2016, 17: 178.
47. Sun R, Chang Y, Yang F, Wang Y, Li H, Zhao Y, Chen D, Wu T, Zhang X, Han Z. A dense SNP genetic map constructed using restriction site-associated DNA sequencing enables detection of QTLs controlling Apple fruit quality. BMC Genomics, 2015, 16: 747.
48. Yu H, Wang J, Zhao Z, Sheng X, Shen Y, Branca F, Gu H. Construction of a High-Density genetic map and identification of LOCI related to hollow stem trait in broccoli (brassic oleracea l. italica). Front Plant Sci, 2019, 10: 45.
49. Shirasawa K, Tanaka M, Takahata Y, Ma D, Cao Q, Liu Q, Zhai H, Kwak SS, Cheol JJ, Yoon UH, Hu LE, Hirakawa H, Isobe S. A high-density SNP genetic map consisting of a complete set of homologous groups in autohexaploid sweetpotato (Ipomoea batatas). Sci Rep, 2017, 7: 44207.
50. Yamaguchi M, Ohtani M, Mitsuda N, Kubo M, Ohme-takagi M, Fukuda H, Demura T. VND-INTERACTING2, a NAC domain transcription factor, negatively regulates xylem vessel formation in Arabidopsis. Plant Cell, 2010, 22(4): 1249-1263.
51. Cao S, Wang Y, Gao Y, Xu R, Ma J, Xu Z, Shang-guan K, Zhang B, Zhou Y. The RLCK-VND6 module coordinates secondary cell wall formation and adaptive growth in rice. Mol Plant, 2023, 16(6): 999-1015.
52. Cong L, Shi YK, Gao XY, Zhao XF, Zhang HQ, Zhou FL, Zhang HJ, Ma BQ, Zhai R, Yang CQ, Wang ZG, Ma FW, Xu LF. Transcription factor PbNAC71 regulates xylem and vessel development to control plant height. Plant Physiol, 2024, 195(1): 395-409.
53. Taylor-teeples M, Lin L, De lucas M, Turco G, Toal TW, Gaudinier A, Young NF, Trabucco GM, Veling MT, Lamothe R, Handakumbura PP, Xiong G, Wang C, Corwin J, Tsoukalas A, Zhang L, Ware D, Pauly M, Kliebenstein DJ, Dehesh K, Tagkopoulos I, Breton G, Pruneda-paz JL, Ahnert SE, Kay SA, Hazen SP, Brady SM. An arabidopsis gene regulatory network for secondary cell wall synthesis. Nature, 2015, 517(7536): 571-575.
54. Nakashima K, Takasaki H, Mizoi J, Shinozaki K, Yamaguchi-shinozaki K. NAC transcription factors in plant abiotic stress responses. Biochim Biophys Acta, 2012, 1819(2): 97-103.
55. Ma QH. Lignin biosynthesis and its diversified roles in disease resistance. Genes (Basel), 2024, 15(3): 295.
56. Liu Q, Luo L, Zheng L. Lignins: biosynthesis and biological functions in plants. Int J Mol Sci, 2018, 19(2): 335.
57. Bang SW, Choi S, Jin X, Jung SE, Choi JW, Seo JS, Kim JK. Transcriptional activation of rice CINNAMOYL-CoA REDUCTASE 10 by OsNAC5, contributes to drought tolerance by modulating lignin accumulation in Roots. Plant Biotechnol J, 2022, 20(4): 736-747.
58. Yuan P, Yang S, Feng L, Chu J, Dong H, Sun J, Chen H, Li Z, Yamamoto N, Zheng A, Li S, Yoon HC, Chen J, Ma D, Xuan YH. Red-light receptor phytochrome B inhibits BZR1-NAC028-CAD8B signaling to negatively regulate rice resistance to sheath blight. Plant Cell Environ, 2023, 46(4): 1249-1263.
59. Huang D, Wang S, Zhang B, Shang-guan K, Shi Y, Zhang D, Liu X, Wu K, Xu Z, Fu X, Zhou Y. A gibberellin-mediated DELLA-NAC signaling cascade regulates cellulose synthesis in rice. Plant Cell, 2015, 27(6): 1681-1696.
60. Yu S, Huang A, Li J, Gao L, Feng Y, Pemberton E, Chen C. OsNAC45 plays complex roles by mediating POD activity and the expression of development-related genes under various abiotic stresses in rice root. Plant Growth Regul, 2018, 84: 519-531.
61. Sun L, Zhang H, Li D, Huang L, Hong Y, Ding XS, Nelson RS, Zhou X, Song F. Functions of rice NAC transcriptional factors, ONAC122 and ONAC131, in defense responses against Magnaporthe grisea. Plant Mol Biol, 2013, 81(1/2): 41-56.
62. Bi Y, Wang H, Yuan X, Yan Y, Li D, Song F. The NAC transcription factor ONAC083 negatively regulates rice immunity against Magnaporthe oryzae by directly activating transcription of the RING-H2 gene OsRFPH2-6. J Integr Plant Biol, 2023, 65(3): 854-875.
63. Wang Z, Xia Y, Lin S, Wang Y, Guo B, Song X, Ding S, Zheng L, Feng R, Chen S, Bao Y, Sheng C, Zhang X, Wu J, Niu D, Jin H, Zhao H. Osa-miR164a targets OsNAC60 and negatively regulates rice immunity against the blast fungus Magnaporthe oryzae. Plant J, 2018, 95(4): 584-597.
64. Wang B, Wei J, Song N, Wang N, Zhao J, Kang Z. A novel wheat NAC transcription factor, TaNAC30, negatively regulates resistance of wheat to stripe rust. J Integr Plant Biol, 2018, 60(5): 432-443.
65. Yang Q, Li B, Rizwan HM, Sun K, Zeng J, Shi M, Guo T, Chen F. Genome-wide identification and comprehensive analyses of NAC transcription factor gene family and expression analysis under Fusarium kyushuense and drought stress conditions in Passiflora edulis. Front Plant Sci, 2022, 13(972734): 页码范围缺失.
66. Ranocha P, Denancé N, Vanholme R, Freydier A, Martinez Y, Hoffmann L, Köhler L, Pouzet C, Renou JP, Sundberg B, Boerjan W, Goffner D. Walls are thin 1 (WAT1), an Arabidopsis homolog of Medicago truncatula NODULIN21, is a tonoplast-localized protein required for secondary wall formation in fibers. Plant J, 2010, 63(3): 469-483.

 doi:10.20944/preprints202410.2200.v1

67. Rao X, Dixon RA. Current models for transcriptional regulation of secondary cell wall biosynthesis in grasses. Front Plant Sci, 2018, 9: 399.
68. Koseoglou E, Hanika K, Mohd NM, Kohlen W, Van der wolf JM, Visser R, Bai Y. Inactivation of tomato WAT1 leads to reduced susceptibility to Clavibacter michiganensis through downregulation of bacterial virulence factors. Front Plant Sci, 2023, 14: 1082094.